Final state interaction effects in electrodisintegration of the deuteron within the Bethe-Salpeter approach

S. G. Bondarenko, V. V. Burov, E. P. Rogochaya¹⁾
Joint Institute for Nuclear Research, 141985 Dubna, Russia

Submitted 12 September 2011.*

The electrodisintegration of the deuteron is considered within a relativistic model of nucleon-nucleon interaction based on the Bethe-Salpeter approach with a separable interaction kernel. The exclusive cross section is calculated within the impulse approximation under various kinematic conditions. Final state interactions between the outgoing nucleons are taken into account. The comparison of nonrelativistic and relativistic calculations is presented. Partial-wave states of the neutron-proton pair with total angular momentum J=0,1 are considered.

1. INTRODUCTION

The electrodisintegration of the deuteron is a useful instrument which makes it possible to investigate the electromagnetic structure of the neutron-proton (np)system. Many approaches have been elaborated to describe this reaction for last 40 years [1–5]. The simplest of them considered the electrodisintegration within a nonrelativistic model of the nucleon-nucleon (NN) interaction and outgoing nucleons were supposed to be free [1] (the plane-wave approximation - PWA). Those approaches were in a good agreement with experimental data at low energies. However, further investigations have shown that the final state interaction (FSI) between outgoing nucleons, two-body currents and other effects should be taken into account to obtain a reasonable agreement with existing experimental data at higher energies. Most of these effects have been considered within nonrelativistic models [2, 3]. In relativistic models, FSI effects could be calculated within quasipotential approaches including the on-mass-shell nucleonnucleon T matrix [4,5].

One of fundamental approaches for a description of the np system is based on using the Bethe-Salpeter (BS) equation [6]. To solve this equation we use a separable ansatz [7] for the NN interaction kernel. In this case, we have to deal with a system of algebraic equations instead of integral ones [8]. A separable kernel model within the BS approach was not used to describe most of high-energy NN processes for a while since calculated expressions contained nonintegrable singularities. The separable kernels proposed in [9–11] make it possible to avoid those difficulties. Using these kernels FSI can be taken into account in the electrodisintegration in a wide range of energy. The electrodisintegration cross section is calculated in the present paper under different

kinematic conditions (see Table 3 below). The rank-six NN interaction potential MY6 [10] is used to describe scattered and bound 3S_1 - 3D_1 partial-wave states. The uncoupled partial-wave states with total angular momentum J=0,1 (1S_0 , 1P_1 , 3P_0 , 3P_1) are described by multirank separable potentials [11]. The obtained results are compared with nonrelativistic model calculations [3] where NN interactions were described by the realistic Paris potential [12].

The paper is organized as follows. In Sec.2., the three-differential cross section of the d(e, e'p)n reaction is considered in the relativistic impulse approximation. The used BS formalism is presented in Sec.3. The details of calculations are considered in Sec.4. Then the obtained relativistic results are compared with nonrelativistic ones [3] and experimental data of the Sacle experiment [13,14] in Sec.5.

2. CROSS SECTION

When all particles are unpolarized the exclusive electrodisintegration of the deuteron d(e,e'p)n can be described by the differential cross section in the deuteron rest frame - laboratory system (LS) - as:

$$\frac{d^{3}\sigma}{dE'_{e}d\Omega'_{e}d\Omega_{p}} = \frac{\sigma_{\text{Mott}}}{8M_{d}(2\pi)^{3}} \frac{\boldsymbol{p}_{p}^{2}\sqrt{s}}{\sqrt{1+\eta}|\boldsymbol{p}_{p}| - E_{p}\sqrt{\eta}\cos\theta_{p}}
\times \left[l_{00}^{0}W_{00} + l_{++}^{0}(W_{++} + W_{--}) + 2l_{+-}^{0}\cos2\phi \text{ Re}W_{+-} \right.
\left. -2l_{+-}^{0}\sin2\phi \text{ Im}W_{+-} - 2l_{0+}^{0}\cos\phi \text{ Re}(W_{0+} - W_{0-}) \right.
\left. -2l_{0+}^{0}\sin\phi \text{ Im}(W_{0+} + W_{0-})\right]. \tag{1}$$

where $\sigma_{\text{Mott}} = (\alpha \cos \frac{\theta}{2}/2E_e \sin^2 \frac{\theta}{2})^2$ is the Mott cross section, $\alpha = e^2/(4\pi)$ is the fine structure constant; M_d is the mass of the deuteron; $q = p_e - p'_e = (\omega, \boldsymbol{q})$ is the momentum transfer; $p_e = (E_e, \boldsymbol{l})$ and $p'_e = (E'_e, \boldsymbol{l}')$ are initial and final electron momenta, respectively; Ω'_e

¹⁾e-mail: rogoch@theor.jinr.ru

is the outgoing electron solid angle; θ is the electron scattering angle. The outgoing proton is described by momentum \boldsymbol{p}_p ($E_p = \sqrt{\boldsymbol{p}_p^2 + m^2}$, m is the mass of the nucleon) and solid angle $\Omega_p = (\theta_p, \phi)$ where θ_p is the zenithal angle between the \boldsymbol{p}_p and \boldsymbol{q} momenta and ϕ is the azimuthal angle between the (ee') and (qp) planes. Factor $\eta = \boldsymbol{q}^2/s$ can be calculated through the np pair total momentum P squared:

$$s = P^2 = (p_p + p_n)^2 = M_d^2 + 2M_d\omega + q^2,$$
 (2)

defined by the sum of the proton p_p and neutron p_n momenta. The photon density matrix elements have the following form:

$$l_{00}^{0} = \frac{Q^{2}}{q^{2}}, \quad l_{0+}^{0} = \frac{Q}{|q|\sqrt{2}}\sqrt{\frac{Q^{2}}{q^{2}}} + \tan^{2}\frac{\theta}{2},$$
$$l_{++}^{0} = \tan^{2}\frac{\theta}{2} + \frac{Q^{2}}{2q^{2}}, \quad l_{+-}^{0} = -\frac{Q^{2}}{2q^{2}},$$
(3)

where $Q^2 = -q^2$ is introduced for convenience. The hadron density matrix elements

$$W_{\lambda\lambda'} = W_{\mu\nu} \varepsilon^{\mu}_{\lambda} \varepsilon^{\nu}_{\lambda'}, \tag{4}$$

where λ , λ' are photon helicity components [15], can be calculated using the photon polarization vectors ε and Cartesian components of hadron tensor

$$W_{\mu\nu} = \frac{1}{3} \sum_{s_d s_n s_p} \left| \langle np : SM_S | j_\mu | d : 1M \rangle \right|^2, \quad (5)$$

where S is the spin of the np pair and M_S is its projection; s_d , s_n and s_p are deuteron, neutron and proton momentum projections, respectively. The matrix element $< np : SM_S|j_\mu|d:1M>$ can be constructed according to the Mandelstam technique [16] and has the following form in LS:

$$< np : SM_S | j_{\mu} | d : 1M > = i \sum_{n=1,2} \int \frac{d^4 p^{\text{CM}}}{(2\pi)^4} \times$$
 (6)

$$\begin{split} & \operatorname{Sp} \left\{ \Lambda(\mathcal{L}^{-1}) \bar{\psi}_{SM_S}(p^{\scriptscriptstyle{\text{CM}}}, p^{*^{\scriptscriptstyle{\text{CM}}}}; P^{\scriptscriptstyle{\text{CM}}}) \Lambda(\mathcal{L}) \Gamma_{\mu}^{(n)}(q) \times \\ & S^{(n)} \left(\frac{K_{(0)}}{2} - (-1)^n p - \frac{q}{2} \right) \Gamma^M \left(p + (-1)^n \frac{q}{2}; K_{(0)} \right) \right\} \end{split}$$

within the relativistic impulse approximation. The sum over n=1,2 corresponds to the interaction of the virtual photon with the proton and with the neutron in the deuteron, respectively. The total P^{CM} and relative $p^{*^{\text{CM}}}$ momenta of the outgoing nucleons and the integration momentum p^{CM} are considered in the final np pair rest frame - center-of-mass system (CM), p denotes

the relative np pair momentum in LS. To perform the integration, momenta p, q and the deuteron total momentum $K_{(0)} = (M_d, \mathbf{0})$ in LS are written in CM using the Lorenz-boost transformation \mathcal{L} along the q direction. The np pair wave function ψ_{SM_S} is transformed from CM to LS by the corresponding boost operator Λ . A detailed description of ψ_{SM_S} , the nth nucleon interaction vertex $\Gamma_{\mu}^{(n)}$, the propagator of the nth nucleon $S^{(n)}$, and the deuteron vertex function Γ^M can be found in our previous works [8,17].

3. SEPARABLE KERNEL OF NN INTERACTION

The outgoing np pair is described by the T matrix which can be found as a solution of the inhomogeneous Bethe-Salpeter equation [6]:

$$T(p', p; P) = V(p', p; P)$$

$$+ \frac{i}{4\pi^3} \int d^4k \, V(p', k; P) \, S_2(k; P) \, T(k, p; P),$$
(7)

where V is the NN interaction kernel, S_2 is the free two-particle Green function:

$$S_2^{-1}(k;P) = \left(\frac{1}{2} \not P + \not k - m\right)^{(1)} \left(\frac{1}{2} \not P - \not k - m\right)^{(2)}, \quad (8)$$

and p (p') is the relative momentum of initial (final) nucleons, P is the total np pair momentum.

To solve the BS equation (7) partial-wave decomposition [18] for the T matrix:

$$T_{\alpha\beta,\gamma\delta}(p',p;P_{(0)}) = \sum_{JMab} t_{ab}(p'_0,|\boldsymbol{p'}|;p_0,|\boldsymbol{p}|;s) \times (9)$$

$$(\mathcal{Y}_{aM}(-\boldsymbol{p'})U_C)_{\alpha\beta}\otimes(U_C\mathcal{Y}_{bM}^{\dagger}(\boldsymbol{p}))_{\delta\gamma}$$

is used. Here $P_{(0)}=(\sqrt{s},\mathbf{0})$ is the np pair total momentum in CM, $U_C=i\gamma^2\gamma^0$ is the charge conjugation matrix. Indices a,b correspond to the set $^{2S+1}L^\rho_J$ of spin S, orbital L and total J angular momenta, $\rho=+$ defines a positive-energy partial-wave state, $\rho=-$ corresponds to a negative-energy one. Greek letters $\{\alpha,\beta,\gamma,\delta\}$ in (9) are used to denote Dirac matrix indices. The spin-angle functions:

$$\mathcal{Y}_{JM:LS\rho}(\mathbf{p})U_{C} = (10)$$

$$i^{L} \sum_{m_{L}m_{S}m_{1}m_{2}\rho_{1}\rho_{2}} C_{\frac{1}{2}\rho_{1}\frac{1}{2}\rho_{2}}^{S_{\rho}\rho} C_{Lm_{L}Sm_{S}}^{JM} C_{\frac{1}{2}m_{1}\frac{1}{2}m_{2}}^{Sm_{S}} \times Y_{Lm_{L}}(\hat{\mathbf{p}})U_{m_{s}}^{\rho_{1}}(1)(\mathbf{p})U_{m_{s}}^{\rho_{2}}(2)^{T}(-\mathbf{p})$$

are constructed from the free nucleon Dirac spinors u, v. It should be mentioned that only positive-energy states with $\rho = +$ are considered in this paper. Using a similar

decomposition for V, the BS equation for radial parts of the T matrix and kernel V is obtained:

$$t_{ab}(p'_0, |\boldsymbol{p'}|; p_0, |\boldsymbol{p}|; s) = v_{ab}(p'_0, |\boldsymbol{p'}|; p_0, |\boldsymbol{p}|; s)$$

$$+ \frac{i}{4\pi^3} \sum_{cd} \int_{-\infty}^{+\infty} dk_0 \int_{0}^{\infty} \boldsymbol{k}^2 d|\boldsymbol{k}| v_{ac}(p'_0, |\boldsymbol{p'}|; k_0, |\boldsymbol{k}|; s)$$

$$\times S_{cd}(k_0, |\boldsymbol{k}|; s) t_{db}(k_0, |\boldsymbol{k}|; p_0, |\boldsymbol{p}|; s).$$
(11)

To solve the resulting equation (11) a separable ansatz [7] for the interaction kernel V is used:

$$v_{ab}(p'_{0}, |\mathbf{p'}|; p_{0}, |\mathbf{p}|; s) = \sum_{i, i=1}^{N} \lambda_{ij}(s) g_{i}^{[a]}(p'_{0}, |\mathbf{p'}|) g_{j}^{[b]}(p_{0}, |\mathbf{p}|),$$
(12)

where N is a rank of a separable kernel, g_i are model functions, λ_{ij} is a parameter matrix. Substituting V (12) in BS equation (7), we obtain the T matrix in a similar separable form:

$$t_{ab}(p'_{0}, |\mathbf{p'}|; p_{0}, |\mathbf{p}|; s) = \sum_{i,j=1}^{N} \tau_{ij}(s) g_{i}^{[a]}(p'_{0}, |\mathbf{p'}|) g_{j}^{[b]}(p_{0}, |\mathbf{p}|)$$
(13)

where:

$$\tau_{ij}(s) = 1/(\lambda_{ij}^{-1}(s) + h_{ij}(s)), \tag{14}$$

and

$$h_{ij}(s) = (15)$$

$$-\frac{i}{4\pi^3} \sum_{a} \int dk_0 \int \mathbf{k}^2 d|\mathbf{k}| \frac{g_i^{[a]}(k_0, |\mathbf{k}|) g_j^{[a]}(k_0, |\mathbf{k}|)}{(\sqrt{s}/2 - E_k + i\epsilon)^2 - k_0^2}$$

are auxiliary functions, $E_{\mathbf{k}} = \sqrt{\mathbf{k}^2 + m^2}$. Thus, the problem of solving the initial integral BS equation (7) turns out to finding the g_i functions and parameters λ_{ij} of separable representation (12). They can be obtained from a description of observables in np elastic scattering [10,11,20–22].

4. FINAL STATE INTERACTION

In our previous works [10, 17] the electrodisintegration of the deuteron was considered within the plane wave approximation (PWA) when the final nucleons were supposed to escape without interaction. Even though PWA is enough to describe the electrodisintegration at low energies, it is important to take into account the final state interaction (FSI) between the outgoing

nucleons. As it was shown in other works [3], the contribution of FSI effects increases with increasing nucleon energies or/and momentum transfer. Therefore, the relativistic models of the NN interaction must be elaborated and FSI should be included into calculations to get an adequate description of the electrodisintegration. The first relativistic model based on a separable kernel approach was Graz II [20]. However, it was impossible in principle to calculate FSI using it [11]. To solve this problem new relativistic separable kernels [10, 11] were elaborated. We apply them to the deuteron electrodisintegration including FSI in this paper.

The outgoing nucleons are described by the BS amplitude which can be written as a sum of two terms:

$$\psi_{SM_S}(p, p^*; P) = \psi_{SM_S}^{(0)}(p, p^*; P)$$

$$+ \frac{i}{4\pi^3} S_2(p; P) \int d^4k \ V(p, k; P) \psi_{SM_S}(k, p^*; P).$$
(16)

The first term

$$\psi_{SM_S}^{(0)}(p, p^*; P) = (2\pi)^4 \chi_{SM_S}(p; P) \delta(p - p^*)$$
 (17)

is related to the outgoing pair of free nucleons (PWA), χ_{SM_S} is a spinor function for two fermions. The second term in (16) corresponds to the final state interaction of the outgoing nucleons. It can be expressed through the T matrix if we use the following relation:

$$\int d^4k \ V(p,k;P)\psi_{SM_S}(k,p^*;P) =$$

$$\int d^4k \ T(p,k;P)\psi_{SM_S}^{(0)}(k,p^*;P)$$
(18)

and can be rewritten as

$$\psi_{SM_S}^{(t)}(p, p^*; P) = (19)$$

$$4\pi i S_2(p; P) T(p, p^*; P) \chi_{SM_S}(p^*; P),$$

here (t) means that this part of the np pair wave function is related to the T matrix. Applying the partial-wave decomposition of the T matrix (9) the expression (19) can be written as follows:

$$\psi_{SM_S}^{(t)}(p, p^*; P) = 4\pi i \times$$

$$\sum_{LmJMa} C_{LmSM_S}^{JM} Y_{Lm}^*(\hat{\boldsymbol{p}}^*) \mathcal{Y}_{aM}(\boldsymbol{p}) \phi_{a,J:LS+}(p_0, |\boldsymbol{p}|; s),$$
(20)

where $p^* = (0, p^*)$ with $|p^*| = \sqrt{s/4 - m^2}$ is the relative momentum of on-mass-shell nucleons in CM, \hat{p}^* denotes the azimuthal angle θ_{p^*} between the p^* and q vectors and zenithal angle ϕ . Since only positive-energy partial-wave states are considered here the radial part is:

$$\phi_{a,J:LS+}(p_0, |\mathbf{p}|; s) = \frac{t_{a,J:LS+}(p_0, |\mathbf{p}|; 0, |\mathbf{p}^*|; s)}{(\sqrt{s}/2 - E_{\mathbf{p}} + i\epsilon)^2 - p_0^2}.$$
 (21)

According to definition (10) spin-angle functions \mathcal{Y} can be written as a product of Dirac γ matrices in the matrix representation [8] as:

$$\mathcal{Y}_{aM}(\mathbf{p}) = \frac{1}{\sqrt{8\pi}} \frac{1}{4E_{\mathbf{p}}(E_{\mathbf{p}} + m)} (m + \mathbf{p}_{1})(1 + \gamma_{0}) \mathcal{G}_{aM}(m - \mathbf{p}_{2}),$$
 (22)

matrices \mathcal{G}_{aM} are given in Table 2. Decomposition (20) is considered in detail in [19]. Using definition (16) and

$a = \left\{ {^{2S+1}L_J^\rho } \right\}$	${\cal G}_{aM}$
${}^{1}S_{0}^{+}$	$-\gamma_5$
${}^{3}S_{1}^{+}$	$_~~ \rlap{\rlap{\rlap{\rlap{\rlap{\rlap{\rlap{\rlap{\rlap{\rlap{\rlap{\rlap{\rlap{\rlap{\rlap{}}}}}}}$
${}^{1}P_{1}^{+}$	$\frac{\sqrt{3}}{ \boldsymbol{p} }(p_1\cdot\xi_M)\gamma_5$
${}^{3}P_{0}^{+}$	$-rac{1}{2 oldsymbol{p} }(oldsymbol{p}_1- oldsymbol{p}_2)$
${}^{3}P_{1}^{+}$	$-\sqrt{\frac{3}{2}}\frac{1}{ \boldsymbol{p} }\left[(p_1\cdot\xi_M)-\frac{1}{2}\boldsymbol{\xi}_M(\boldsymbol{p}_1-\boldsymbol{p}_2)\right]\gamma_5$
$^{3}D_{1}^{+}$	$\frac{1}{\sqrt{2}} \left[\xi_M + \frac{3}{2} \frac{1}{\boldsymbol{p}^2} (p_1 \cdot \xi_M) (\boldsymbol{p}_1 - \boldsymbol{p}_2) \right]$

Spin-angular parts \mathcal{G}_{aM} (22) for the np pair; $p_1 = (E_p, \mathbf{p}), p_2 = (E_p, -\mathbf{p})$ are on-mass-shell momenta, $E_p = \sqrt{\mathbf{p}^2 + m^2}$; γ matrices are defined as in [23].

substituting (17), (20) into (6), the final expression for hadron current $< np : SM_S|j_{\mu}|d : 1M > \text{can be obtained}$. It consists of two parts. One of them:

$$\langle np : SM_{S} | j_{\mu} | d : 1M \rangle^{(0)} =$$

$$i \sum_{n=1,2} \left\{ \Lambda(\mathcal{L}^{-1}) \bar{\chi}_{SM_{S}} \left(p^{*^{\text{CM}}}; P^{\text{CM}} \right) \Lambda(\mathcal{L}) \Gamma_{\mu}^{(n)}(q) \times \right.$$

$$S^{(n)} \left(\frac{K_{(0)}}{2} - (-1)^{n} p^{*} - \frac{q}{2} \right) \Gamma^{M} \left(p^{*} + (-1)^{n} \frac{q}{2}; K_{(0)} \right) \right\}$$

corresponds to the electrodisintegration in PWA. Another one:

$$\langle np : SM_{S}|j_{\mu}|d : 1M \rangle^{(t)} =$$

$$\frac{i}{4\pi^{3}} \sum_{n=1,2} \sum_{LmJM_{J}L'lm'} C_{LmSM_{S}}^{JM_{J}} Y_{Lm}(\hat{\boldsymbol{p}}^{*}) \times$$

$$\int_{-\infty}^{\infty} dp_{0}^{\text{CM}} \int_{0}^{\infty} (\boldsymbol{p}^{\text{CM}})^{2} d|\boldsymbol{p}^{\text{CM}}| \int_{-1}^{1} d\cos\theta_{\boldsymbol{p}}^{\text{CM}} \int_{0}^{2\pi} d\phi \times$$

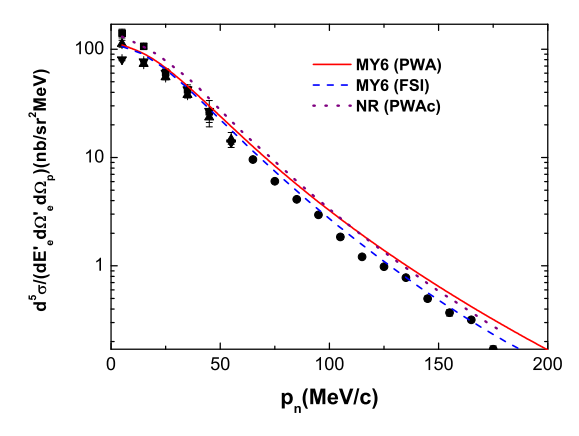
$$\operatorname{Sp} \left\{ \Lambda(\mathcal{L}^{-1}) \bar{\mathcal{Y}}_{JL'SM_{J}}(\boldsymbol{p}^{\text{CM}}) \Lambda(\mathcal{L}) \Gamma_{\mu}^{(n)}(q) \times$$

$$S^{(n)} \left(\frac{K_{(0)}}{2} - (-1)^{n} p - \frac{q}{2} \right) \mathcal{Y}_{1lSm'} \left(\boldsymbol{p} + (-1)^{n} \frac{\boldsymbol{q}}{2} \right) \right\} \times$$

$$\frac{t_{L'L}^{*}(p_{0}^{\text{CM}}, |\boldsymbol{p}^{\text{CM}}|; 0, |\boldsymbol{p}^{*}|; s)}{(\sqrt{s}/2 - E_{\boldsymbol{p}} + i\epsilon)^{2} - p_{0}^{2}} \times$$

$$g_{l} \left(p_{0} + (-1)^{n} \frac{\omega}{2}, \boldsymbol{p} + (-1)^{n} \frac{\boldsymbol{q}}{2}; K_{(0)} \right)$$

corresponds to the process when FSI is taken into account. Here g_l is a radial part of the deuteron vertex function Γ^M . The part Sp $\{...\}$ has been calculated using the algebra manipulation package MAPLE. The three-dimensional integration over p_0^{CM} , $|\boldsymbol{p}^{\text{CM}}|$ and $\cos\theta_p^{\text{CM}}$ has been performed numerically using the programming language FORTRAN.



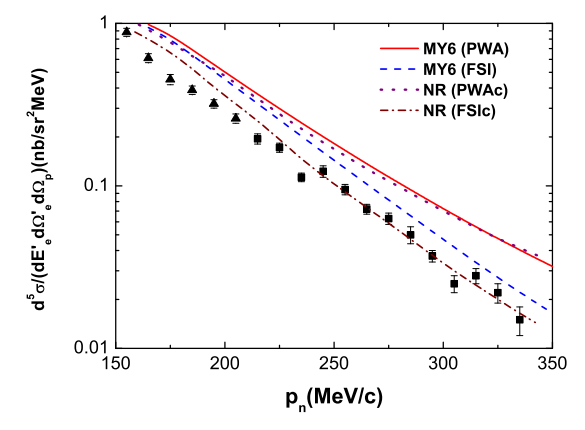
Cross section (1) depending on recoil neutron momentum $|\boldsymbol{p}_n|$ calculated under kinematic conditions set I of the Sacle experiment [13]. The notations are following: MY6 (PWA) (red solid line) - relativistic calculation in the plane-wave approximation with the MY6 potential [10]; MY6 (FSI) (blue dashed line) - relativistic calculation including FSI effects; NR (PWAc) (violet dotted line) - nonrelativistic calculation [3].

5. RESULTS AND DISCUSSION

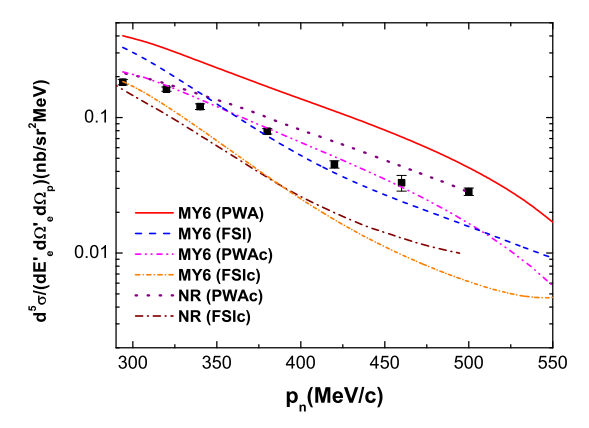
The differential cross section (1) is calculated under three kinematic conditions of the Sacle experiment [13,14] (described in Table 3) and is present in Figs.1-3.

		set I [13]	set II [13]	[14]
E_e , GeV		0.500	0.500	0.560
E'_e , GeV		0.395	0.352	0.360
θ, °		59	44.4	25
$\boldsymbol{p}_n,\mathrm{GeV}/c$	min	0.005	0.165	0.294
	max	0.350	0.350	0.550
θ_n , °	min	101.81	172.07	153.01
	max	37.78	70.23	20.81
$\theta_{qe},{}^{\circ}$	min	48.79	44.74	33.06
$\boldsymbol{p}_p,\mathrm{GeV}/c$	min	0.451	0.514	0.557
	max	0.276	0.403	0.306
$\theta_p,$ $^{\circ}$	min	0.622	2.54	13.86
	max	51.03	54.90	140.28
$\theta_{pe},^{\circ}$	min	49.41	47.28	46.92
	max	99.81	99.64	173.35
\sqrt{s} , GeV		1.929	1.993	2.057
$\sqrt{s} - 2m$, GeV		0.051	0.115	0.176
Q^2 , $(\text{GeV}/c)^2$		0.192	0.101	0.038
ω , GeV		0.105	0.148	0.200
q , GeV/ c		0.450	0.350	0.279

Kinematic conditions considered in the paper. Here all quantities are in LS. In addition to those which are defined in the text, they are: angle θ_{qe} between the beam and the virtual photon; neutron momentum \boldsymbol{p}_n and angle θ_n between the neutron and the virtual photon $(\boldsymbol{p}_p, \theta_p$ – the same for the proton); θ_{pe} (θ_{qe}) – the angle between the beam and the proton (virtual photon).



The same as in Fig.1 but under kinematic conditions set II of the Sacle experiment [13]. The nonrelativistic calculation NR (FSIc) (brown dashed-dotted line) includes FSI effects.



The same as in Figs.1,2 but under kinematic conditions of the Sacle experiment [14]. Two additional results are presented for comparison: MY6 (PWAc) (pink dashed-dotted-dotted line) - relativistic PWA calculation; MY6 (FSIc) (orange dashed-dotted line) - relativistic calculation with FSI effects; both obtained under current conservation condition (25).

The calculations have been performed within the relativistic impulse approximation for two different cases: when the outgoing nucleons are supposed to be free (PWA) and when the final state interaction between the nucleons is taken into account (FSI). The partial-wave states of the np pair with total angular momentum J=0,1 have been considered. The used relativistic model consists of two parts: the separable potential MY6 [10] for the bound (deuteron) and scattered 3S_1 - 3D_1 states and separable potentials of various ranks [11] - for all the other partial-wave states (1S_0 , 1P_1 , 3P_0 , 3P_1). The obtained results have been compared with the nonrelativistic model [3].

In Fig.1, relativistic MY6 (PWA), MY6 (FSI) and nonrelativistic NR (PWAc) calculations under kinematic conditions [13] (set I) are practically coincide with each other and go close to the experimental data. The notation "c" in NR (PWAc) means that the corresponding hadron current satisfies the current conservation condition [1]:

$$q^{\mu}J_{\mu} = 0. \tag{25}$$

So, it can be concluded that relativistic and FSI effects do not play an important role in description of the deuteron electrodisintegration at low energies.

Fig.2 considers the cross section (1) calculated under kinematic conditions [13] (set II). Here FSI effects decrease the resulting cross section noticeably. A slight difference is seen between nonrelativistic and relativistic results.

The cross section under kinematic conditions [14] is presented in Fig.3. In this case PWA and FSI calculations differ significantly. It means that the influence of FSI on observables increases with increasing $|p_n|$. To investigate relativistic effects, two additional calculations MY6 (PWAc), MY6 (FSIc) have been performed when the condition (25) has been taken into account. The relativistic one-particle current within the impulse approximation (6) does not satisfy (25). We impose this condition on the hadron current (23), (24) as it was done in [3] for a nonrelativistic model to compare our relativistic result with it and investigate relativistic effects. It has been done only under kinematic conditions [14] since an influence of the current conservation condition becomes significant at high outgoing neutron momenta $|p_n|$. The comparison of MY6 (PWAc) and NR (PWAc), MY6 (FSIc) and NR (FSIc) demonstrates that relativistic effects become significant with increasing $|\boldsymbol{p}_n|$. FSI effects decrease the obtained cross section.

As it is seen from the figures, an influence of FSI increases with increasing outgoing neutron momentum $|p_n|$. FSI effects are significant at outgoing neutron momenta $|\boldsymbol{p}_n| > 150 \,\mathrm{MeV/c}$ even at low momentum transfer. It has been demonstrated that the FSI contribution always decreases the value of the cross section (1). From present results it can also be seen that the FSI contribution relatively to the PWA one is approximately the same both for nonrelativistic and relativistic models. However, other effects, like negative-energy partial-wave states and two-body currents, should be taken into account for further conclusions. It should be also emphasized that the relativistic calculation of FSI has been performed within the BS approach using a relativistic separable potential for the first time. Recently the considered separable potentials [10, 11] have been modified to take into account inelastic processes (production of various mesons) occurring in the NN interaction at high energies [22]. However, energies of nucleons do not reach the inelasticity threshold under kinematic conditions [13]. The inelasticity effects are nonzero under conditions [14] but they are conjectured to be small in this case.

- 1. T. De Forest, Nucl. Phys. A392, 232 (1983).
- 2. H. Arenhovel, Nucl. Phys. A384, 287 (1982).
- A.Yu. Korchin, Yu.P. Melnik, and A.V. Shebeko, Sov. J. Nucl. Phys. 48, 243 (1988).
- G.I. Gakh, A.P. Rekalo, and E. Tomasi-Gustafsson, Annals Phys. 319, 150 (2005).
- S. Jeschonnek and J.W. Van Orden, Phys. Rev. C78, 014007 (2008).

- E.E. Salpeter and H.A. Bethe, Phys. Rev. 84, 1232 (1951).
- Y. Yamaguchi, Phys. Rev. 95, 1628 (1954);
 Y. Yamaguchi and Y. Yamaguchi, Phys. Rev. 95, 1635 (1954).
- S.G. Bondarenko, V.V. Burov, A.V. Molochkov, G.I. Smirnov, and H. Toki, Prog. Part. Nucl. Phys. 48, 449 (2002).
- S.G. Bondarenko, V.V. Burov, W-Y. Pauchy Hwang, and Rogochaya, E.P., JETP Lett. 87, 653 (2008).
- S.G. Bondarenko, V.V. Burov, W.-Y.Pauchy Hwang, and E.P. Rogochaya, Nucl. Phys. A848, 75 (2010).
- S.G. Bondarenko, V.V. Burov, W.-Y. Pauchy Hwang, and E.P. Rogochaya, Nucl. Phys. A832, 233 (2010).
- 12. M. Lacombe et al. Phys. Rev. C21, 861 (1980).
- 13. M. Bernheim et al., Nucl. Phys. A365, 349 (1981).
- 14. S. Turck-Chieze et al., Phys. Lett. **B142**, 145 (1984).
- V. Dmitrasinovic and F. Gross, Phys. Rev. C40, 2479 (1989).
- S. Mandelstam, Proc. Roy. Soc. Lond. A233, 248 (1955).
- S.G. Bondarenko, V.V. Burov, E.P. Rogochaya, and A.A. Goy, Phys. Part. Nucl. Lett. 2, 323 (2005);
 S.G. Bondarenko, V.V. Burov, E.P. Rogochaya, and A.A. Goy, Phys. Atom. Nucl. 70, 2054 (2007).
- 18. J.J. Kubis, Phys. Rev. **D6**, 547 (1972).
- 19. S.G. Bondarenko, V.V. Burov, K.Yu. Kazakov, and D.V. Shulga, Phys. Part. Nucl. Lett. 1, 178 (2004).
- 20. G. Rupp and J.A. Tjon, Phys. Rev. C41, 472 (1990).
- L. Mathelitsch, W. Plessas, and W. Schweiger, Phys. Rev. C26, 65 (1982).
- S.G. Bondarenko, V.V. Burov, and E.P. Rogochaya, preprint 1106.4478 [nucl-th], doi:10.1016/j.physletb.2011.10.009; preprint 1108.4170 [nucl-th], doi:10.1016/j.nuclphysbps.2011.10.081.
- J.D. Bjorken and S.D. Drell, Relativistic Quantum Mechanics and Relativistic Quantum Fields. McGraw-Hill, New York (1964).